WSI Applied Remote Sensing and Analysis

January 4, 2013

# USFS Region 5 LiDAR

## Northern California Delivery 1
## Technical Data Report


Bret Hazell
3Di West
3400 W 11th Ave.
Eugene, OR 97402
bhazell@3diwest.com
PH: 541-343-8877

WSI Corvallis Office
517 SW 2nd St., Suite 400
Corvallis, OR 97333
PH: 541-752-1204

# TABLE OF CONTENTS



**Cover Photo:** View looking north at the Taliaferro Ridge Landslide in the Mendocino National Forest, California. Image created from the LiDAR point cloud colored by 2010 NAIP imagery.

# INTRODUCTION

View of the project area in Northern California showing a mixed conifer landscape.

In August 2012, WSI (Watershed Sciences, Inc.) was contracted by3Di West, in conjunction with the USDA Forest Service (USFS), to collect Light Detection and Ranging (LiDAR) data for multiple areas throughout USFS Region 5, including sites in the Inyo, Mendocino, Klamath, Shasta-Trinity, Six Rivers, Sierra, and Sequoia National Forests. The LiDAR data were collected to aid in identifying ecological restoration opportunities by assessing forest structural complexity, mapping geomorphic features, and quantifying acreages of highly suitable wildlife habitat.

This report accompanies the first delivered LiDAR data set for 5 areas of interest (AOIs) in the Klamath, Mendocino, Shasta-Trinity, and Six Rivers National Forests (Figure 1) and documents data acquisition procedures, processing methods, and results of all accuracy assessments. Project specifics for this delivery are shown in Table 1, and a complete list of contracted deliverables provided to 3Di West can be found in Table 2.

**Table 1: Acquisition dates, acreages, and data types collected on the USFS Region 5 LiDAR site.**

| Project Site | Contracted Acres | Buffered Acres | Acquisition Dates | Data Type |
|---|---|---|---|---|
| **Snag Hill** | 25,425 | 26,456 | 10/14/2012 | LiDAR |
| **Mule** | 10,653 | 11,445 | 10/15/2012 | |
| **Taliaferro** | 5,230 | 5,688 | 10/16/2012 | |
| **Trout Creek** | 3,706 | 4,105 | 10/16/2012 | |
| **Marble Valley** | 6,697 | 7,220 | 10/17/2012 | |

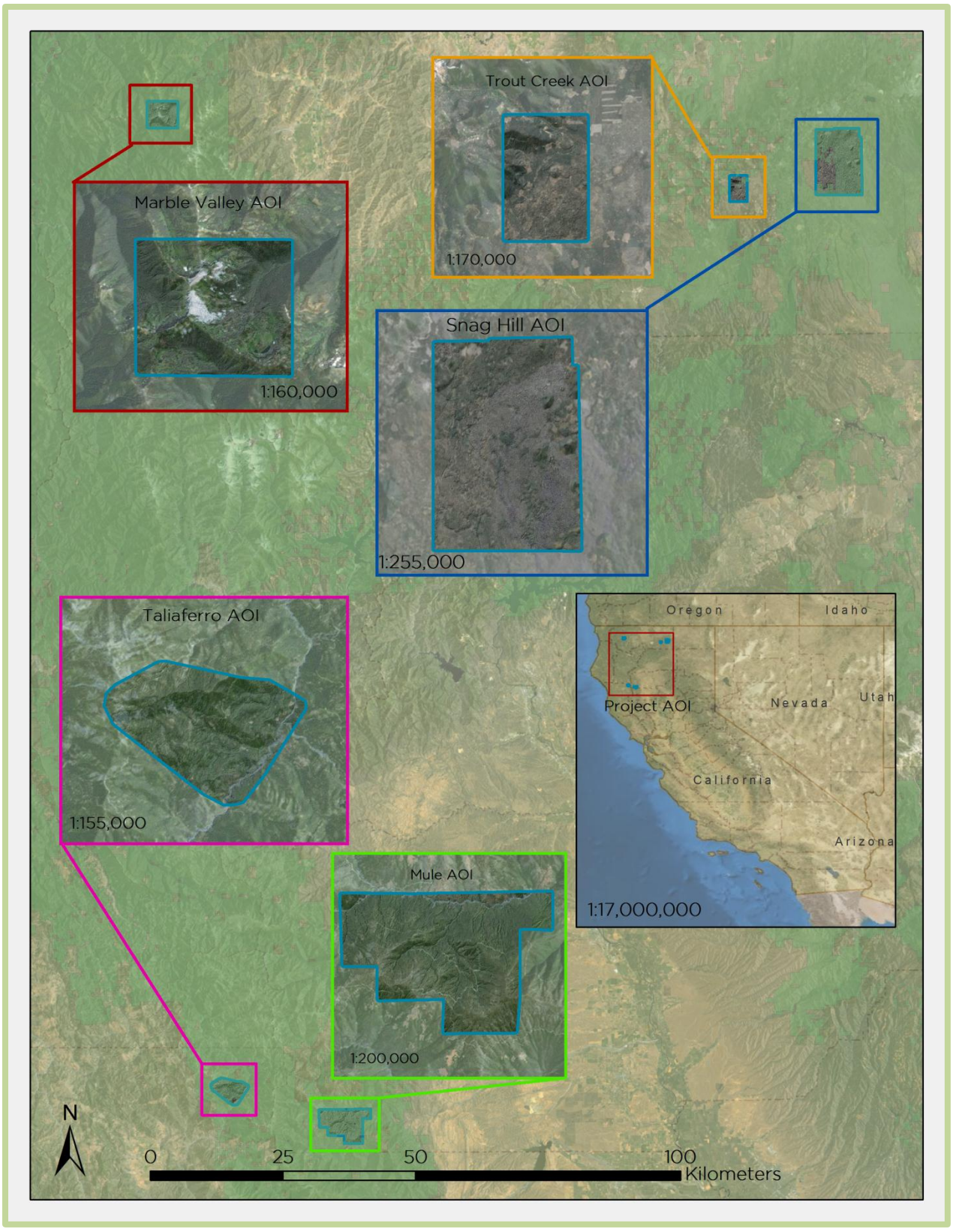


**Figure 1: Location map of the delivered USFS Region 5 LiDAR sites in Northern California**

**Table 2: Products delivered to 3Di West for the 5 Northern California AOIs**

| Projection: UTM Zone 10 North<br>Horizontal Datum: NAD83 (CORS96)<br>Vertical Datum: NAVD88 (GEOID03)<br>Units: Meters | |
|---|---|
| **LAS Files** | LAS v 1.2<br>• All Returns |
| **Rasters** | 1 Meter ESRI Grids and GeoTiffs<br>• Bare Earth Model<br>• Highest Hit Model<br>1 Meter GeoTiffs<br>• Intensity Images |
| **Vectors** | Shapefiles (*.shp)<br>• Site Boundary<br>• LiDAR Index<br>• DEM/DSM Index<br>• Smooth Best Estimate Trajectory (SBETs)<br>Geodatabase (*.gdb)<br>• Ground points |

Leica ALS50 LiDAR sensor installation

# Planning

In preparation for data collection, WSI reviewed the project area using Google Earth, and flightlines were developed using ALTM-NAV Planner (v.3.0) software. Careful planning by acquisition staff entailed adapting the pulse rate, flight altitude, scan angle, and ground speed to ensure complete coverage of the LiDAR study areas at the target point density of ≥8 pulses per square. Efforts are taken to optimize flight paths by minimizing flight times while meeting all accuracy specifications.

Factors such as satellite constellation availability and weather windows must be considered. Any weather hazards and conditions affecting the flight were continuously monitored due to their impact on the daily success of airborne and ground operations. In addition, a variety of logistical considerations require review: private property access, potential air space restrictions, and availability of company resources (both staff and equipment). Significant effort was made to acquire all LiDAR areas with no snow on the ground. Acquisition of the Bluff Creek, Slides Glade, Deadman Creek, Moores Flat Hyd Mine, and Michigan Bluff Hyd Mine AOIs are still outstanding and acquisition is dependent on snow melt.

# Ground Survey


Ground survey data is used to geospatially correct the aircraft positional coordinate data and to perform quality assurance checks on the final LiDAR data. Ground professionals set permanent survey monuments and collect real time kinematic (RTK) surveys to support the airborne acquisition process.

## Monumentation

The spatial configuration of ground survey monuments provided redundant control within 13 nautical miles of the mission areas for LiDAR flights. Monuments were also used for collection of ground control points using RTK survey techniques. Monument locations were selected with consideration for satellite visibility, field crew safety, and optimal location for RTK coverage. WSI occupied 4 existing monuments and established 17 new monuments for the Northern California area of the survey (Table 3, Figure 2). New monumentation was set using 5/8”x30” rebar topped with stamped 2" aluminum caps.

To correct the continuous onboard measurements of the aircraft position recorded throughout the missions, WSI concurrently conducted multiple static Global Navigation Satellite System (GNSS) ground surveys (1 Hz recording frequency) over each monument. After the airborne survey, the static GPS data were triangulated with nearby Continuously Operating Reference Stations (CORS) using the Online Positioning User Service (OPUS[1]) for precise positioning. Multiple independent sessions over the same monument were processed to confirm antenna height measurements and to refine position accuracy.

## RTK Surveys

For the real time kinetic (RTK) check point data collection, a Trimble R7 base unit was positioned at a nearby monument to broadcast a kinematic correction to a roving Trimble R8 GNSS receiver. All RTK measurements were made during periods with a Position Dilution of Precision (PDOP) of ≤ 3.0 with at least six satellites in view of the stationary and roving receivers. When collecting RTK data, the rover would record data while stationary for five seconds, then calculate the pseudorange position using at least three one-second epochs. Relative errors for the position must be less than 1.5 cm horizontal and 2.0 cm vertical in order to be accepted.

RTK positions were collected on paved roads and other hard surface locations such as gravel or stable dirt roads that also had good satellite visibility. RTK measurements were not taken on highly reflective surfaces such as center line stripes or lane markings on roads due to the increased noise seen in the laser returns over these surfaces. The distribution of RTK points depended on ground access constraints and may not be equitably distributed throughout the study area. The Marble Valley AOI was inaccessible for RTK; therefore, care was taken to fly over the nearest RTK area during the aerial acquisition. See Figure 2 for the distribution of RTK in this project.

All static surveys were collected with Trimble model R7 GNSS receivers equipped with a Zephyr Geodetic Model 2 RoHS antenna. A Trimble model R8 GNSS receiver was used to collect RTK. All GNSS measurements were made with dual frequency L1-L2 receivers with carrier-phase correction. See Table 4 for Trimble unit specifications.

[1] OPUS is a free service provided by the National Geodetic Survey to process corrected monument positions. http://www.ngs.noaa.gov/OPUS.

**Table 3: Monuments established for the Region 5 Northern California LiDAR acquisitions. Coordinates are on the NAD83 (CORS96) datum, epoch 2002.00**

| Monument ID | Latitude | Longitude | Ellipsoid (meters) |
|---|---|---|---|
| DH6531 | 40 53 15.88630 | -123 36 11.10993 | 156.970 |
| KS0531 | 39 56 32.59114 | -120 57 12.33373 | 1018.021 |
| MINE_01 | 39 56 56.24662 | -121 03 03.59741 | 1094.058 |
| LU2289 | 40 39 07.51122 | 122 56 30.81067 | 478.731 |
| SR_01 | 41 27 02.52108 | -121 52 32.03918 | 1470.597 |
| SR_02 | 41 31 35.63127 | -121 41 44.86339 | 1695.548 |
| SR_03 | 39 49 39.58161 | -122 47 31.77964 | 1559.476 |
| SR_04 | 39 48 12.33448 | -122 42 55.00367 | 1491.586 |
| SR_05 | 39 50 04.16363 | -123 05 18.19365 | 695.993 |
| SR_06 | 39 53 16.37281 | -123 05 22.51151 | 1396.186 |
| SR_07 | 40 02 18.04320 | -122 49 15.44311 | 1975.587 |
| SR_08 | 40 03 46.55717 | -122 44 34.19431 | 1650.324 |
| SR_09 | 41 36 32.44346 | -122 58 11.88728 | 818.723 |
| SR_10 | 41 36 54.97991 | -122 58 13.09310 | 809.815 |
| SR_11 | 39 54 24.71837 | -123 01 40.75106 | 934.195 |
| SR_12 | 40 51 01.75635 | -123 33 27.97462 | 494.596 |
| SR_13 | 40 50 19.94893 | -123 43 13.00377 | 1451.809 |
| SR_14 | 40 47 14.59291 | -123 41 07.21712 | 1564.425 |
| SR_15 | 40 40 21.70425 | -123 35 57.95568 | 1476.592 |
| SR_17 | 40 37 41.89450 | -123 28 16.44261 | 353.581 |
| SR_18 | 40 42 02.18201 | -123 31 48.96728 | 544.815 |

**Table 4: Trimble equipment identification**

| Receiver Model | Antenna | OPUS Antenna ID | Use |
|---|---|---|---|
| Trimble R7 GNSS | Zephyr GNSS Geodetic Model 2 | TRM57971.00 | Static |
| Trimble R8 | Integrated Antenna R8 Model 2 | TRM_R8_GNSS | RTK |

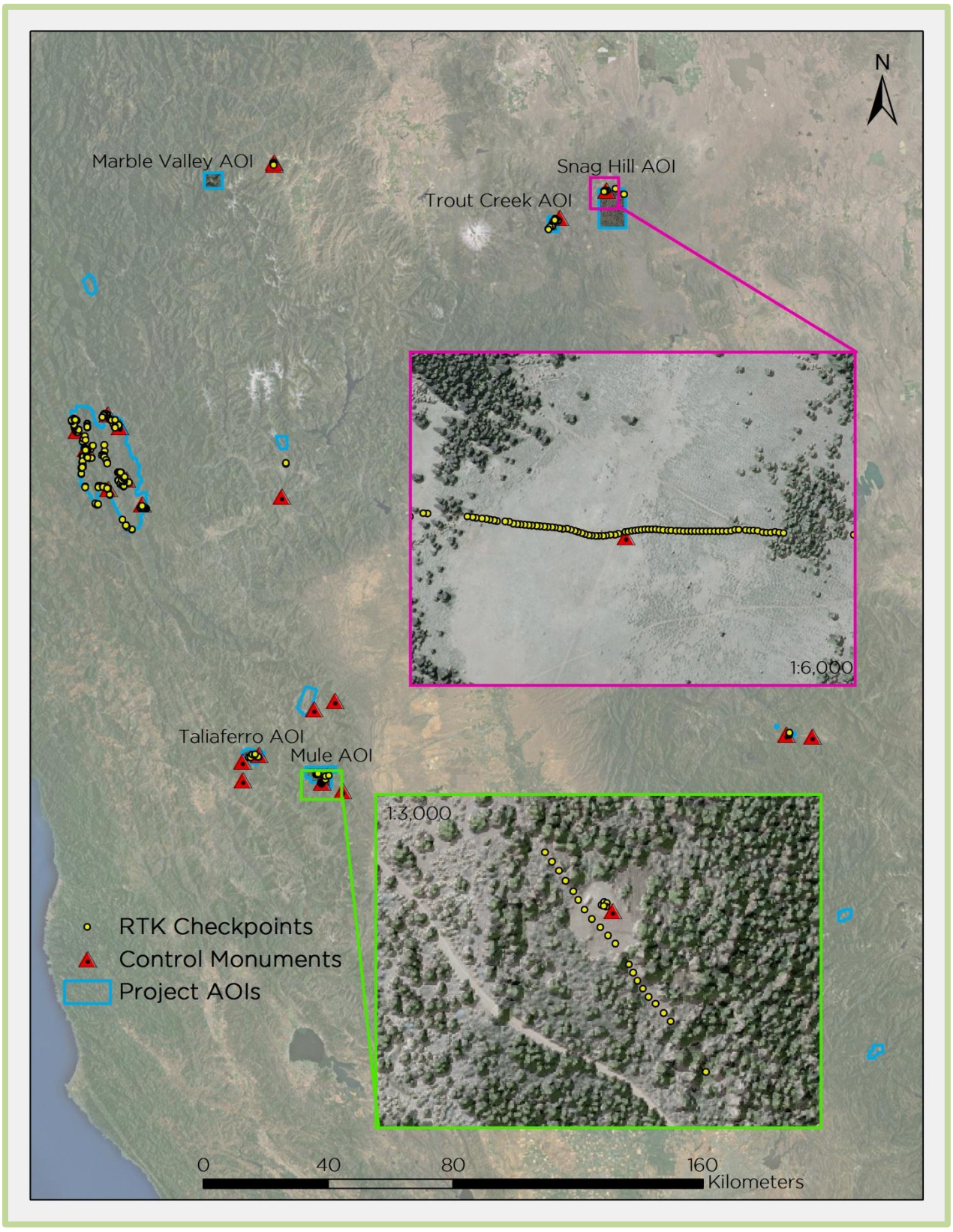


**Figure 2: Basestation and RTK checkpoint location map**

# Airborne Survey

## LiDAR

The LiDAR survey was accomplished with a Leica ALS50 Phase II system mounted in a Cessna Caravan. Table 5 summarizes the settings used to yield an average pulse density of ≥8 pulses/$m^2$ over the USFS Region 5 LiDAR terrain. It is not uncommon for some types of surfaces (e.g. dense vegetation or water) to return fewer pulses to the LiDAR sensor than the laser originally emitted. These discrepancies between native and delivered density will vary depending on terrain, land cover, and the prevalence of water bodies.

**Table 5: LiDAR survey settings and specifications for all delivered LiDAR AOIs**

| LiDAR Survey Settings & Specifications | |
|---|---|
| Sensor | Leica ALS50 |
| Survey Altitude (AGL) | 900 m |
| Target Pulse Rate | 98-105 kHz |
| Sensor Configuration | Single Pulse in Air (SPiA) |
| Laser Pulse Diameter | 21 cm |
| Mirror Scan Rate | 52.2 Hz |
| Field of View | 30° |
| GPS Baselines | ≤13 nm |
| GPS PDOP | ≤3.0 |
| GPS Satellite Constellation | ≥6 |
| Maximum Returns | 4 |
| Intensity | 8-bit |
| Resolution/Density | Average 8 pulses/$m^2$ |
| Accuracy | $RMSE_Z$ ≤ 15 cm |

To reduce laser shadowing and increase surface laser painting, all areas were surveyed with an opposing flight line side-lap of ≥50% (≥100% overlap). The Leica laser systems record up to four range measurements (returns) per pulse. All discernible laser returns were processed for the output dataset.

To accurately solve for laser point position (geographic coordinates x, y, z), the positional coordinates of the airborne sensor and the attitude of the aircraft were recorded continuously throughout the LiDAR data collection mission. Position of the aircraft was measured twice per second (2 Hz) by an onboard differential GPS unit. Aircraft attitude was measured 200 times per second (200 Hz) as pitch, roll, and yaw (heading) from an onboard inertial measurement unit (IMU). To allow for post-processing correction and calibration, aircraft/sensor position and attitude data are indexed by GPS time.

View looking west over the lakes of Sky High Valley near Black Marble Mountain in the Klamath National Forest. Image created from the LiDAR point cloud colored by 2010 NAIP imagery.

# LiDAR Data

Upon the LiDAR data's arrival to the office, WSI processing staff initiates a suite of automated and manual techniques to process the data into the requested deliverables. Processing tasks include GPS control computations, kinematic corrections, calculation of laser point position, calibration for optimal relative and absolute accuracy, and classification of ground and non-ground points (Table 6). Processing methodologies are tailored for the landscape and intended application of the point data. A full description of these tasks can be found in Table 7.

**Table 6: ASPRS LAS classification standards applied to the USFS Region 5 LiDAR dataset**

| Classification Number | Classification Name | Classification Description |
|---|---|---|
| 1 | Default/ Unclassified | Laser returns that are not included in the ground class and not dismissed as Noise or Withheld points. |
| 2 | Ground | Ground that is determined by a number of automated and manual cleaning algorithms to determine the best ground model the data can support. |
| 7 | Noise | Low points and/or noise |
| 11 | Withheld | Laser returns that have intensity values of 0 or 255 |

**Table 7: LiDAR processing workflow**

| LiDAR Processing Step | Software Used |
|---|---|
| Resolve kinematic corrections for aircraft position data using kinematic aircraft GPS and static ground GPS data. | Waypoint GPS v.8.3<br>Trimble Business Center v.2.80<br>Blue Marble Desktop v.2.5 |
| Develop a smoothed best estimate of trajectory (SBET) file that blends post-processed aircraft position with attitude data. Sensor head position and attitude are calculated throughout the survey. The SBET data are used extensively for laser point processing. | IPAS TC v.3.1 |
| Calculate laser point position by associating SBET position to each laser point return time, scan angle, intensity, etc. Create raw laser point cloud data for the entire survey in *.las (ASPRS v. 1.2) format. Data are converted to orthometric elevations (NAVD88) by applying a Geoid12 correction. | ALS Post Processing Software v.2.74 |
| Import raw laser points into manageable blocks (less than 500 MB) to perform manual relative accuracy calibration and filter erroneous points. Ground points are then classified for individual flight lines (to be used for relative accuracy testing and calibration). | TerraScan v.12.004 |
| Using ground classified points per each flight line, the relative accuracy is tested. Automated line-to-line calibrations are then performed for system attitude parameters (pitch, roll, heading), mirror flex (scale) and GPS/IMU drift. Calibrations are calculated on ground classified points from paired flight lines and results are applied to all points in a flight line. Every flight line is used for relative accuracy calibration. | TerraMatch v.12.001 |
| Classify resulting data to ground and other client designated ASPRS classifications (Table 6). Assess statistical absolute accuracy via direct comparisons of ground classified points to ground RTK survey data. | TerraScan v.12.004<br>TerraModeler v.12.002 |
| Generate bare earth models as triangulated surfaces. Highest hit models were created as a surface expression of all classified points (excluding the noise and withheld classes). All surface models were exported as GeoTIFFs at a 1 meter pixel resolution. | TerraScan v.12.004<br>ArcMap v. 10.0<br>TerraModeler v.12.002 |

View looking southeast at Chimney Crater near Snag Hill in the Shasta - Trinity National Forest. Image created from the LiDAR-derived bare-earth Model colored by elevation.

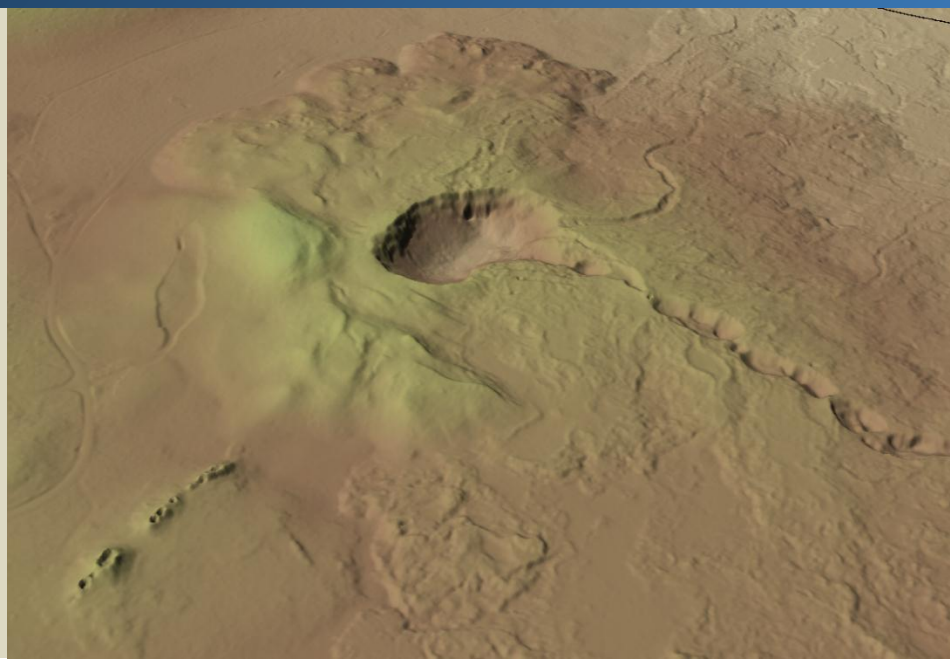

# LiDAR Density

The average cumulative first-return density for the delivered AOIs was 15.57 points/$m^2$ (Table 8). The pulse density distribution will vary within the study area due to laser scan pattern and flight conditions. Additionally, some types of surfaces (i.e. breaks in terrain, water, steep slopes) may return fewer pulses to the sensor (delivered density) than originally emitted by the laser (native density).

The statistical distribution of cumulative first returns (Figure 3) and cumulative classified ground points (Figure 4) are portrayed below. Also presented are the spatial distribution of average first return densities (Figure 5) and ground point densities (Figure 6) for each 100 $m^2$ cell. Statistical histograms for individual AOIs can be seen in Appendix A.

**Table 8: Average LiDAR point densities**

| Point Density (points/$m^2$) | | | | | | |
|---|---|---|---|---|---|---|
| **AOI** | **Cumulative** | **Snag Hill** | **Mule** | **Taliaferro** | **Trout Creek** | **Marble Valley** |
| First-Return | 15.57 | 9.662 | 15.23 | 13.82 | 9.58 | 13.50 |
| Ground Classified | 1.72 | 2.23 | 1.78 | 2.31 | 2.28 | 2.04 |

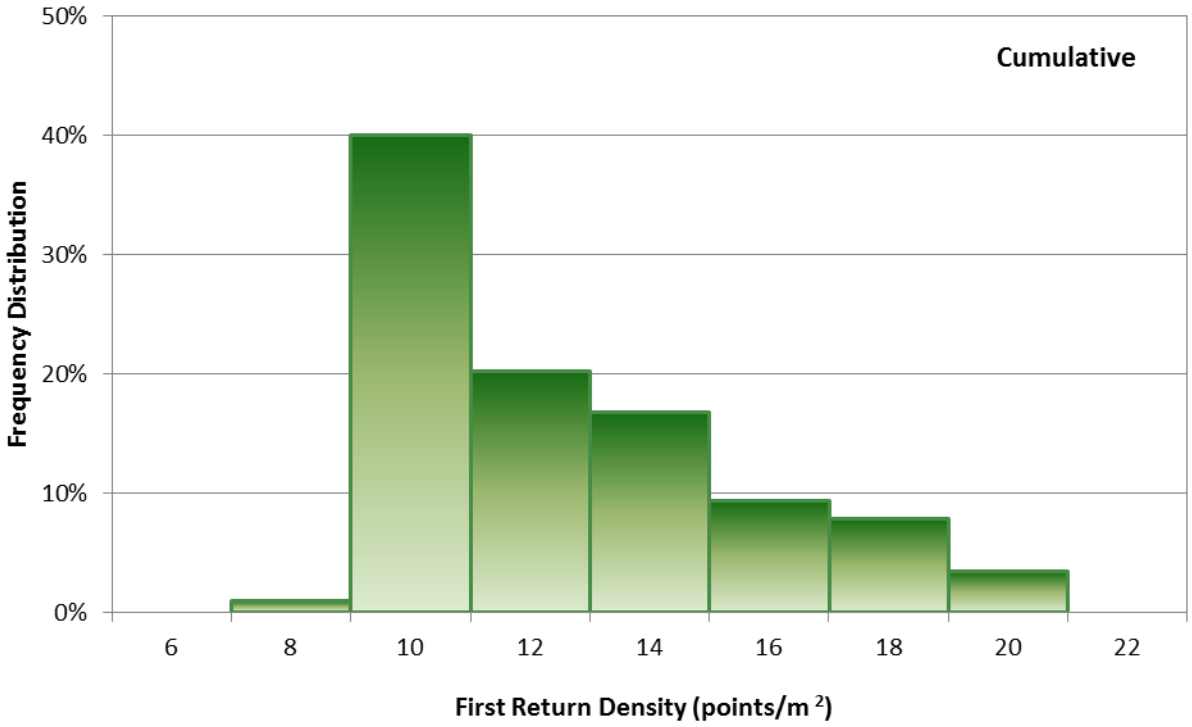


**Figure 3: Frequency distribution of first return densities (native densities) of the 1m gridded study area for all 5 delivered AOIs**

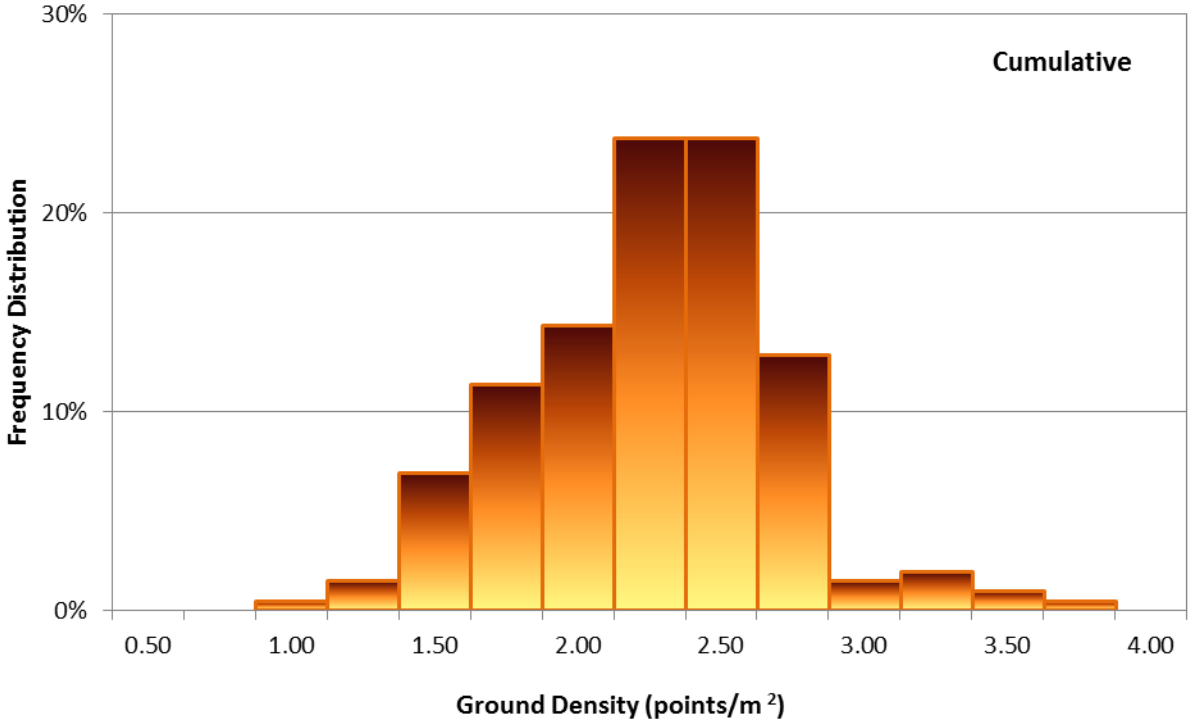


**Figure 4: Frequency distribution of ground return densities of the 1m gridded study area for all 5 delivered AOIs**

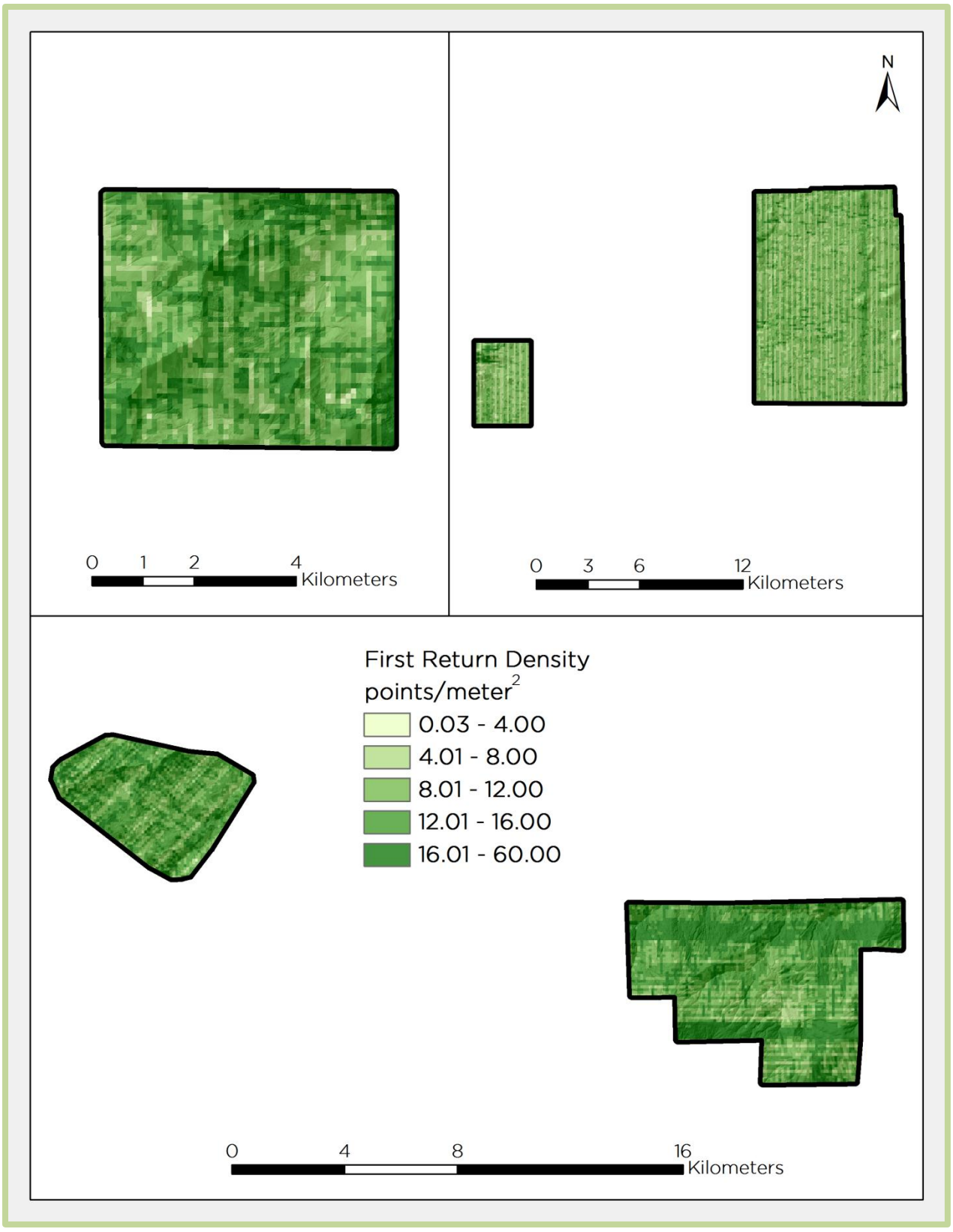


**Figure 5: Native density map for the delivered Northern California AOIs**

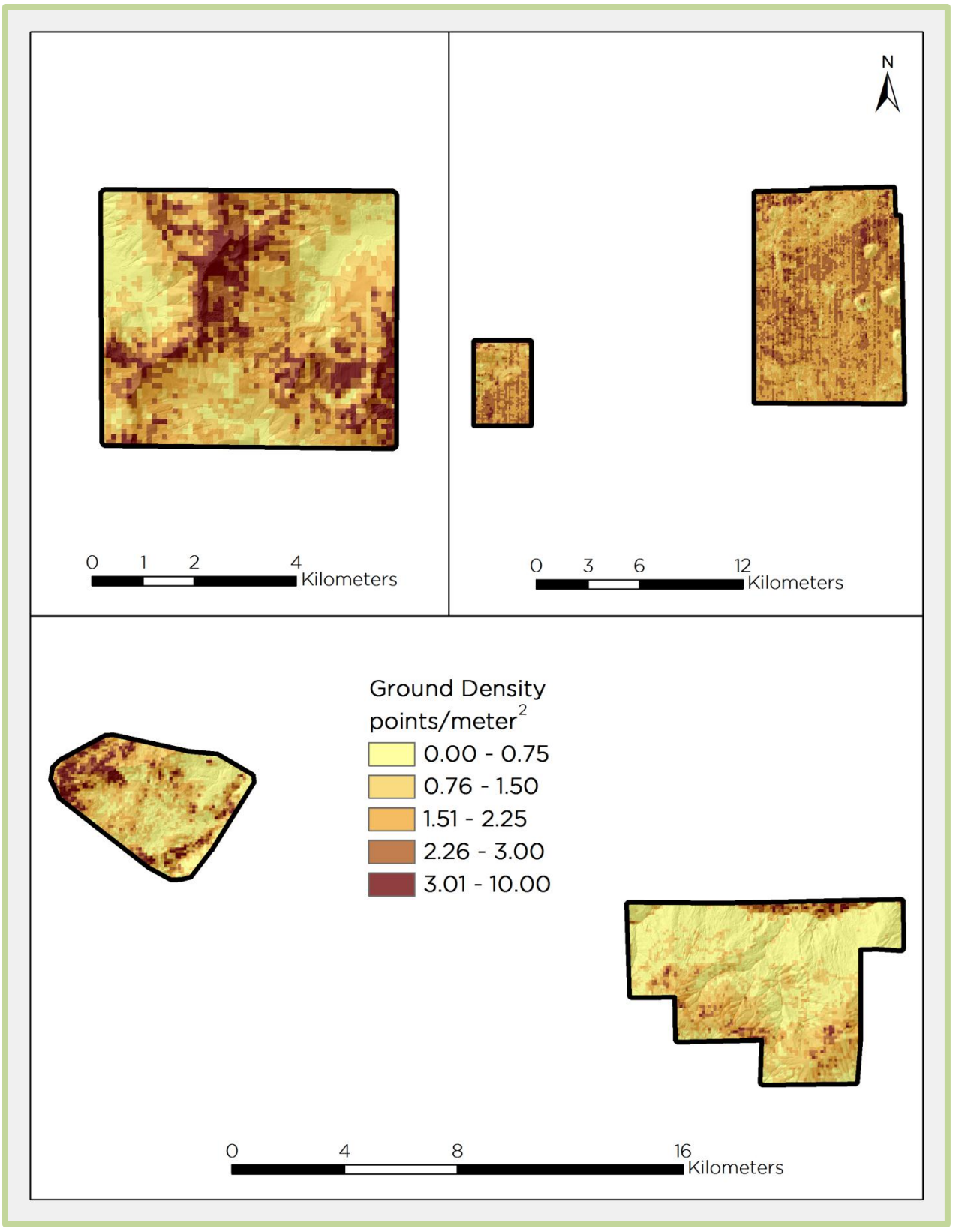


**Figure 6: Ground density map for the delivered Northern California AOIs**

# LiDAR Accuracy Assessments

The accuracy of LiDAR data collection can be described in terms of absolute accuracy (the consistency of the data with external data sources) and relative accuracy (the consistency of the dataset with itself).

## LiDAR Absolute Accuracy

Vertical absolute accuracy was primarily assessed from RTK ground check point (GCP) data collected on open, bare earth surfaces with level slope (<20°). Fundamental Vertical Accuracy (FVA) reporting is designed to meet guidelines presented in the National Standard for Spatial Data Accuracy (FGDC, 1998). FVA compares known RTK ground survey check points to the triangulated ground surface generated by the LiDAR points. FVA is a measure of the accuracy of LiDAR point data in open areas where the LiDAR system has a "very high probability" of measuring the ground surface and is evaluated at the 95% confidence interval (1.96 $\sigma$).

Absolute accuracy is described as the mean and standard deviation (sigma $\sigma$) of divergence of the ground surface model from ground survey point coordinates. These statistics assume the error for x, y, and z is normally distributed, and therefore the skew and kurtosis of distributions are also considered when evaluating error statistics. For the delivered AOIs, 662 RTK ground check points were collected in total resulting in an average accuracy of -0.004 meters (Table 9, Figure 7). Because RTK ground check points are not distributed evenly throughout the AOIs, individual AOI absolute accuracies were not calculated.

**Table 9: Cumulative absolute accuracy statistics**

| Absolute Accuracy | Cumulative |
|---|---|
| Sample | 662 points |
| Average | -0.004 m |
| Median | -0.003 m |
| RMSE | 0.030 m |
| 1σ | 0.030 m |
| 2σ | 0.059 m |

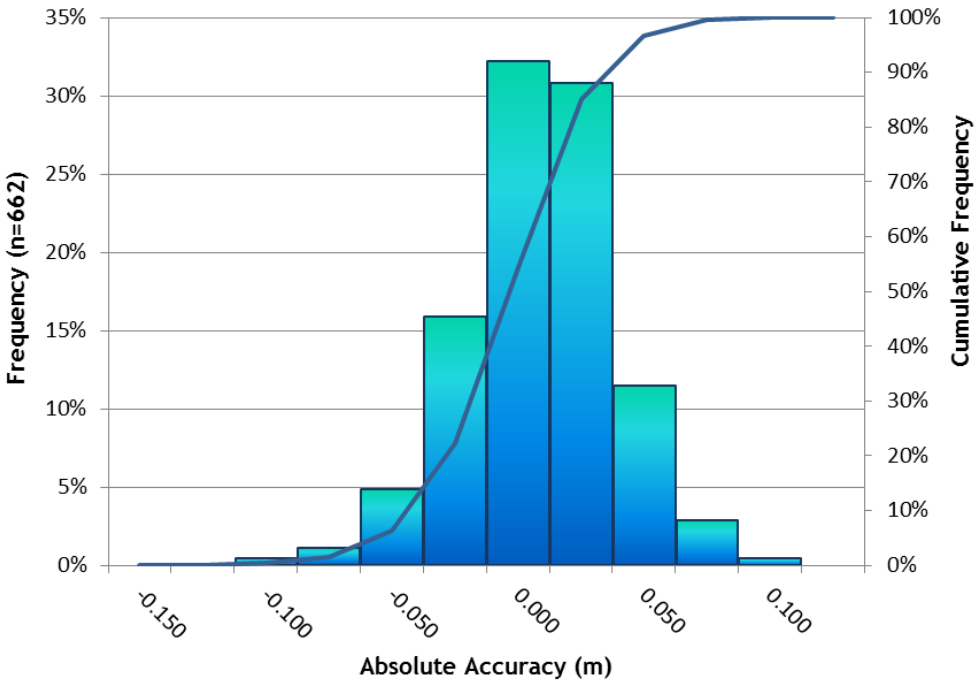


**Figure 7: Frequency histogram for LiDAR surface deviation from RTK values**

# LiDAR Relative Accuracy

Relative accuracy refers to the internal consistency of the data set as a whole: the ability to place an object in the same location given multiple flight lines, GPS conditions, and aircraft attitudes. When the LiDAR system is well calibrated, the swath-to-swath divergence is low (<0.10 meters). The relative accuracy is computed by comparing the ground surface model of each individual flight line with its neighbors in overlapping regions. The average relative accuracy for the delivered AOIs was 0.022 meters (Table 10, **Figure** 8). Frequency plots by individual AOI can be seen in Appendix B. See Appendix C for further information on sources of error and operational measures used to improve relative accuracy.

**Table 10: Relative accuracy (in meters) by AOI**

| Absolute Accuracy | Cumulative | Snag Hill | Mule | Taliaferro | Trout Creek | Marble Valley |
|---|---|---|---|---|---|---|
| Sample Size | 255 surfaces | 55 surfaces | 65 surfaces | 57 surfaces | 22 surfaces | 56 surfaces |
| Average (m) | 0.022 | 0.018 | 0.025 | 0.027 | 0.016 | 0.027 |
| Median (m) | 0.024 | 0.019 | 0.025 | 0.026 | 0.016 | 0.027 |
| RMSE (m) | 0.025 | 0.019 | 0.026 | 0.028 | 0.016 | 0.027 |
| 1σ (m) | 0.005 | 0.003 | 0.004 | 0.004 | 0.001 | 0.003 |
| 1.96σ (m) | 0.011 | 0.005 | 0.007 | 0.008 | 0.002 | 0.006 |

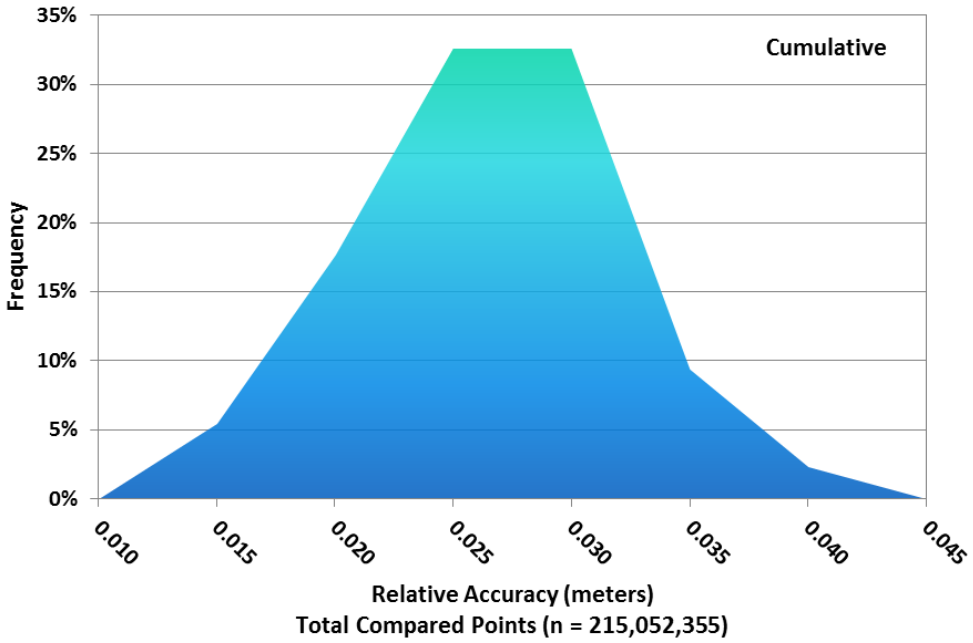


**Figure 8: Frequency plot for relative accuracy between flight lines across all delivered AOIs**

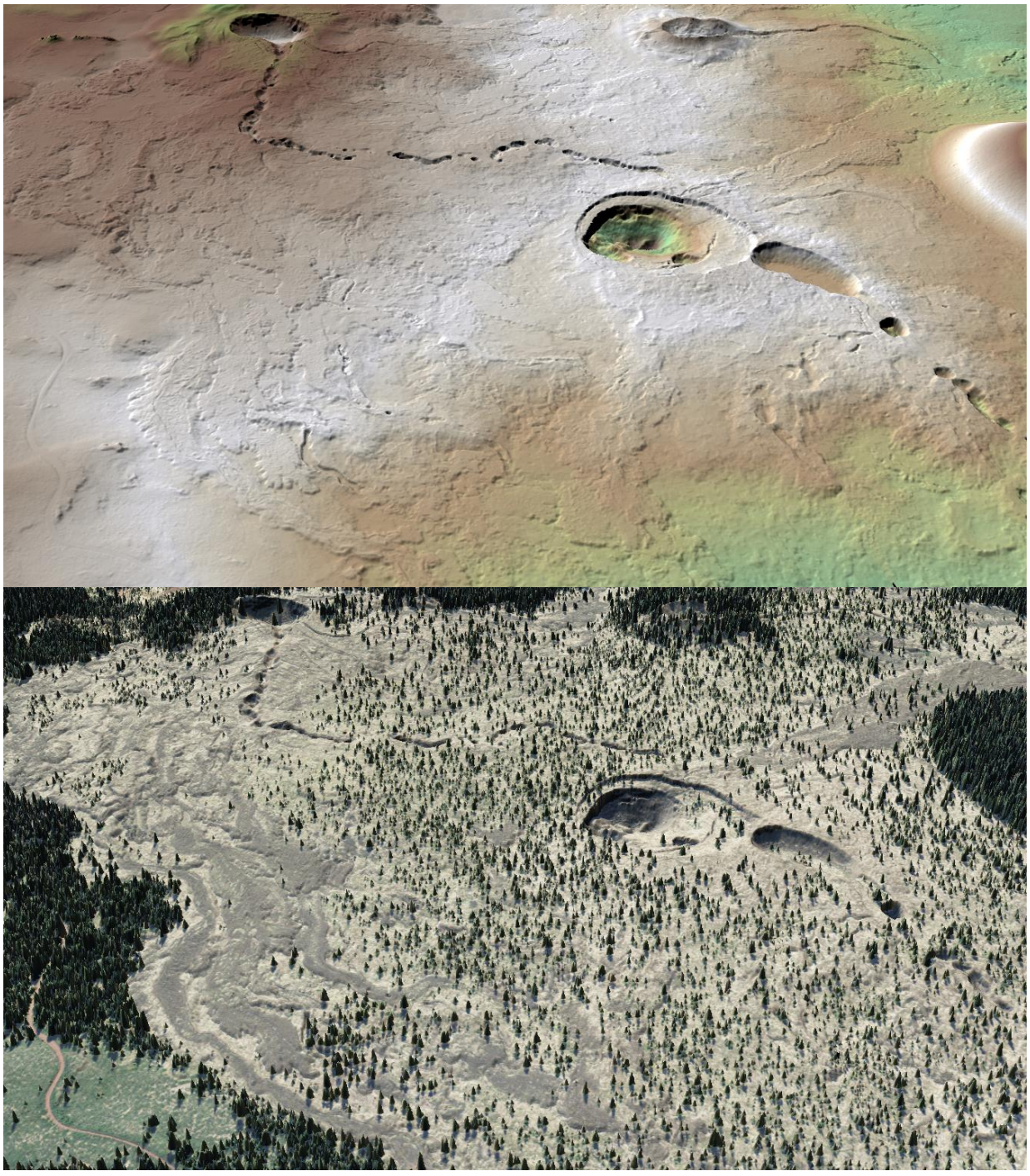

**Figure 9: View looking east over a lava flow showing Chimney and Giant Craters near Snag Hill in the Shasta-Trinity National Forest. Top image created from the LiDAR-derived bare-earth Model colored by elevation with the lower image from the highest-hit model colored by 2010 NAIP imagery.**

**Figure 10: View looking south over Black Marble Mountain toward Marble Valley in the Klamath National Forest. Image created from the LiDAR point cloud colored by 2010 NAIP imagery.**

**Figure 11: View looking north at Snag Hill in Shasta-Trinity National Forest. Image created from the LiDAR point cloud colored by 2010 NAIP imagery.**

# GLOSSARY

**1-sigma (σ) Absolute Deviation:** Value for which the data are within one standard deviation (approximately 68$^{th}$ percentile) of a normally distributed data set.

**1.96-sigma (σ) Absolute Deviation:** Value for which the data are within two standard deviations (approximately 95$^{th}$ percentile) of a normally distributed data set.

**Root Mean Square Error (RMSE):** A statistic used to approximate the difference between real-world points and the LiDAR points. It is calculated by squaring all the values, then taking the average of the squares and taking the square root of the average.

**Pulse Rate (PR)**: The rate at which laser pulses are emitted from the sensor; typically measured as thousands of pulses per second (kHz).

**Pulse Returns**: For every laser pulse emitted, the Leica ALS 60 system can record *up to four* wave forms reflected back to the sensor. Portions of the wave form that return earliest are the highest element in multi-tiered surfaces such as vegetation. Portions of the wave form that return last are the lowest element in multi-tiered surfaces.

**Accuracy**: The statistical comparison between known (surveyed) points and laser points. Typically measured as the standard deviation (sigma σ) and root mean square error (RMSE).

**Intensity Values**: The peak power ratio of the laser return to the emitted laser. It is a function of surface reflectivity.

**Data Density**: A common measure of LiDAR resolution, measured as points per square meter.

**Spot Spacing**: Also a measure of LiDAR resolution, measured as the average distance between laser points.

**Nadir**: A single point or locus of points on the surface of the earth directly below a sensor as it progresses along its flight line.

**Scan Angle**: The angle from nadir to the edge of the scan, measured in degrees. Laser point accuracy typically decreases as scan angles increase.

**Overlap**: The area shared between flight lines, typically measured in percent; 100% overlap is essential to ensure complete coverage and reduce laser shadows.

**DTM / DEM**: These often-interchanged terms refer to models made from laser points. The digital elevation model (DEM) refers to all surfaces, including bare ground and vegetation, while the digital terrain model (DTM) refers only to those points classified as ground.

**Real-Time Kinematic (RTK) Survey**: GPS surveying is conducted with a GPS base station deployed over a known monument with a radio connection to a GPS rover. Both the base station and rover receive differential GPS data and the baseline correction is solved between the two. This type of ground survey is accurate to 1.5 cm or less.

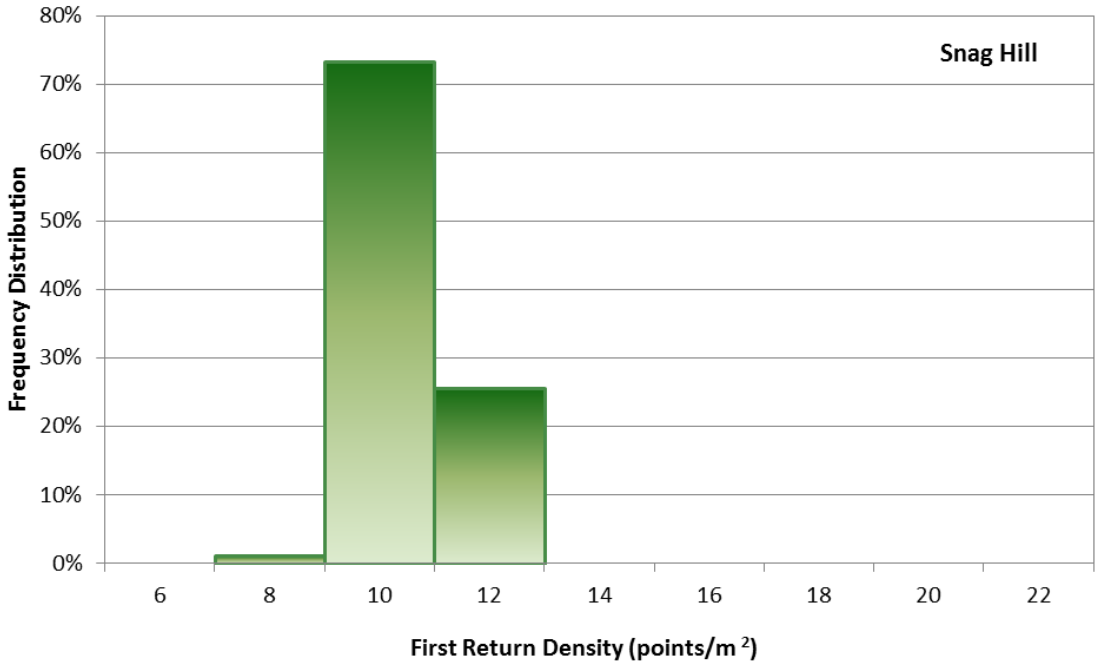


**Frequency distribution of first return densities (native densities) of the 1m gridded study area for the Snag Hill AOI**

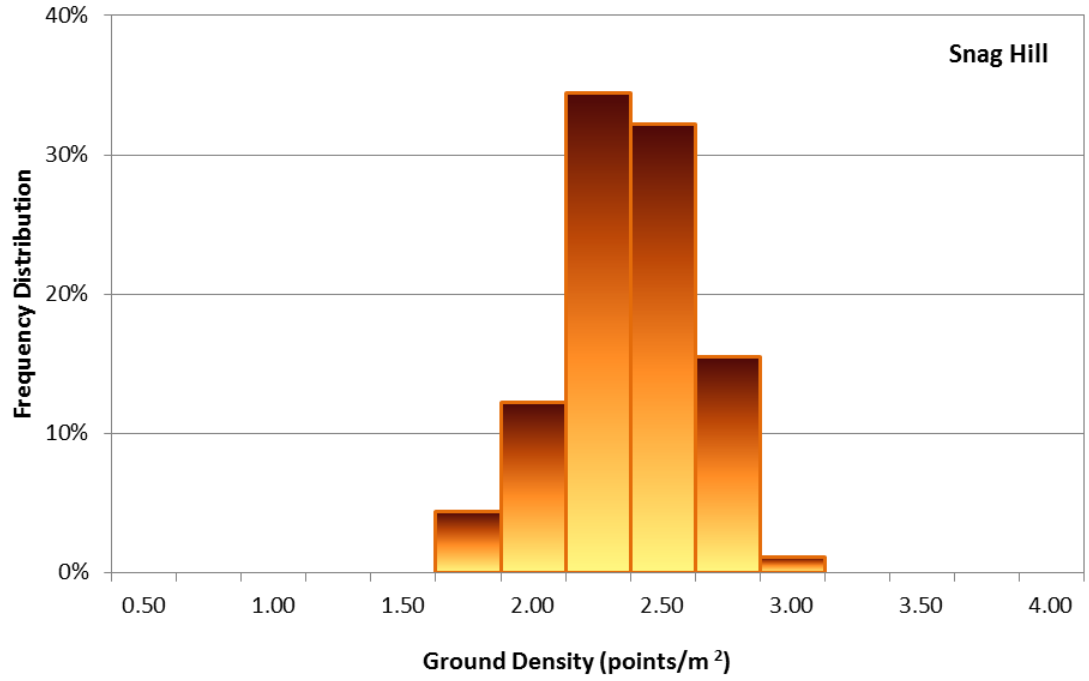


**Frequency distribution of ground return densities of the 1m gridded study area for the Snag Hill AOI**

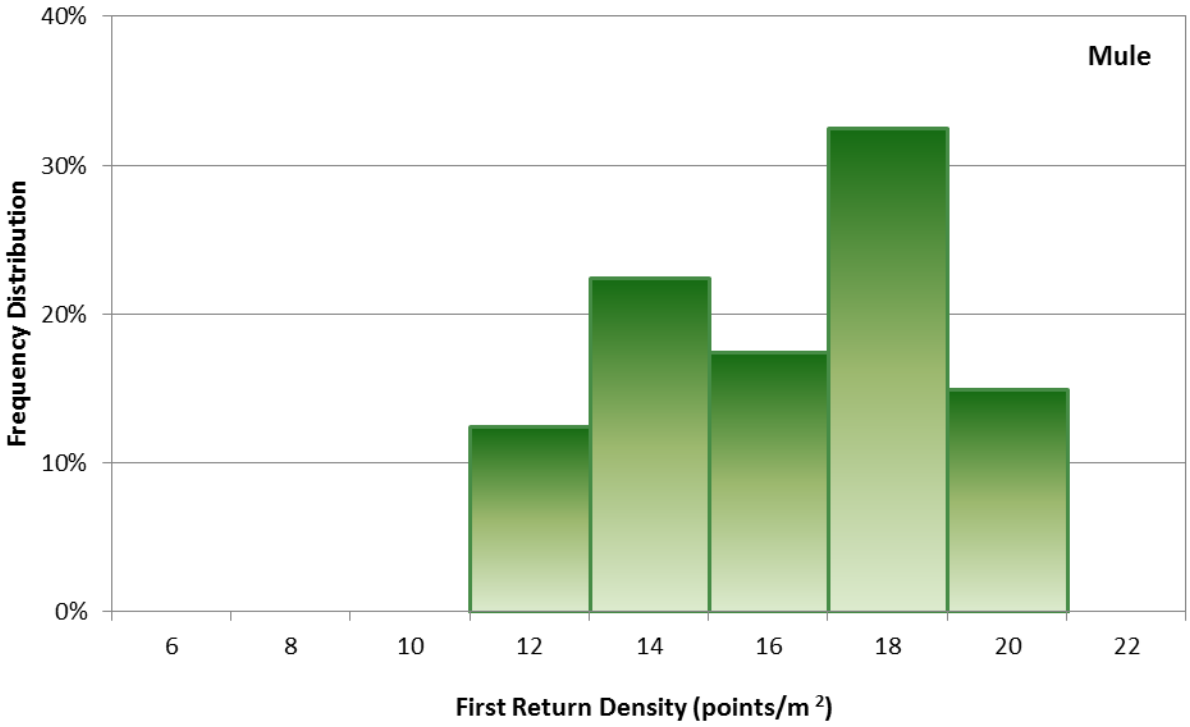


**Frequency distribution of first return densities (native densities) of the 1m gridded study area for the Mule AOI**

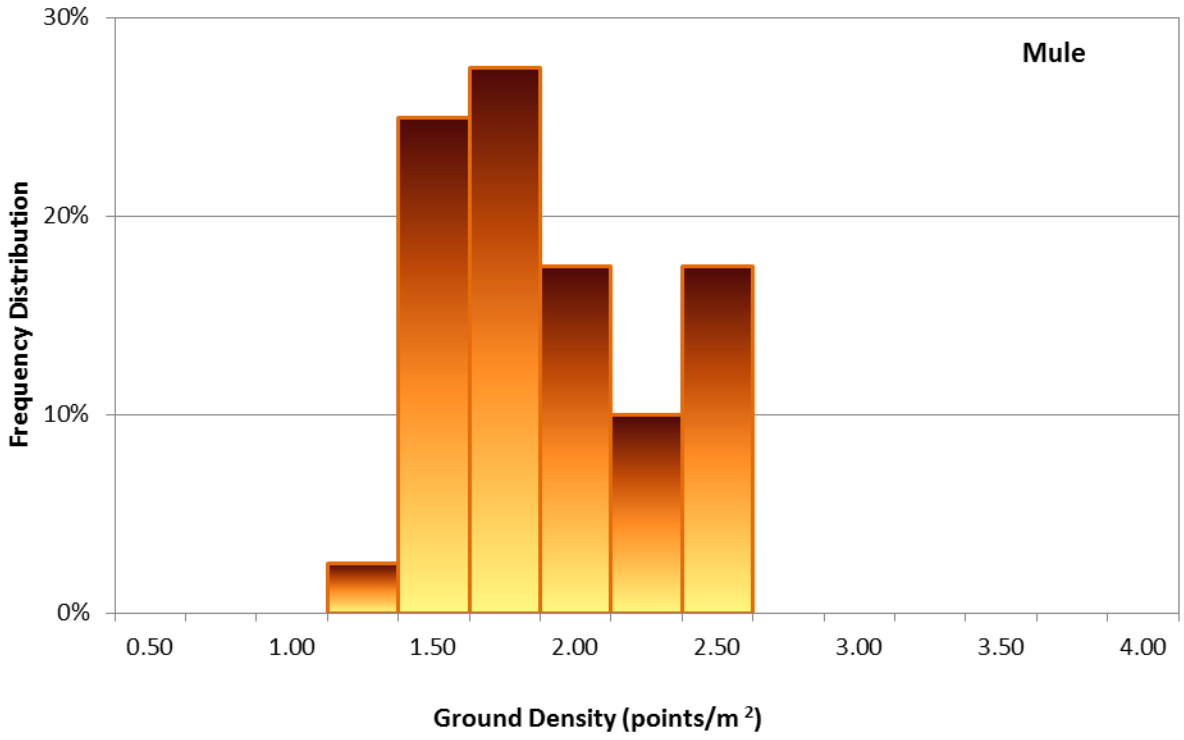


**Frequency distribution of ground return densities of the 1m gridded study area for the Mule AOI**

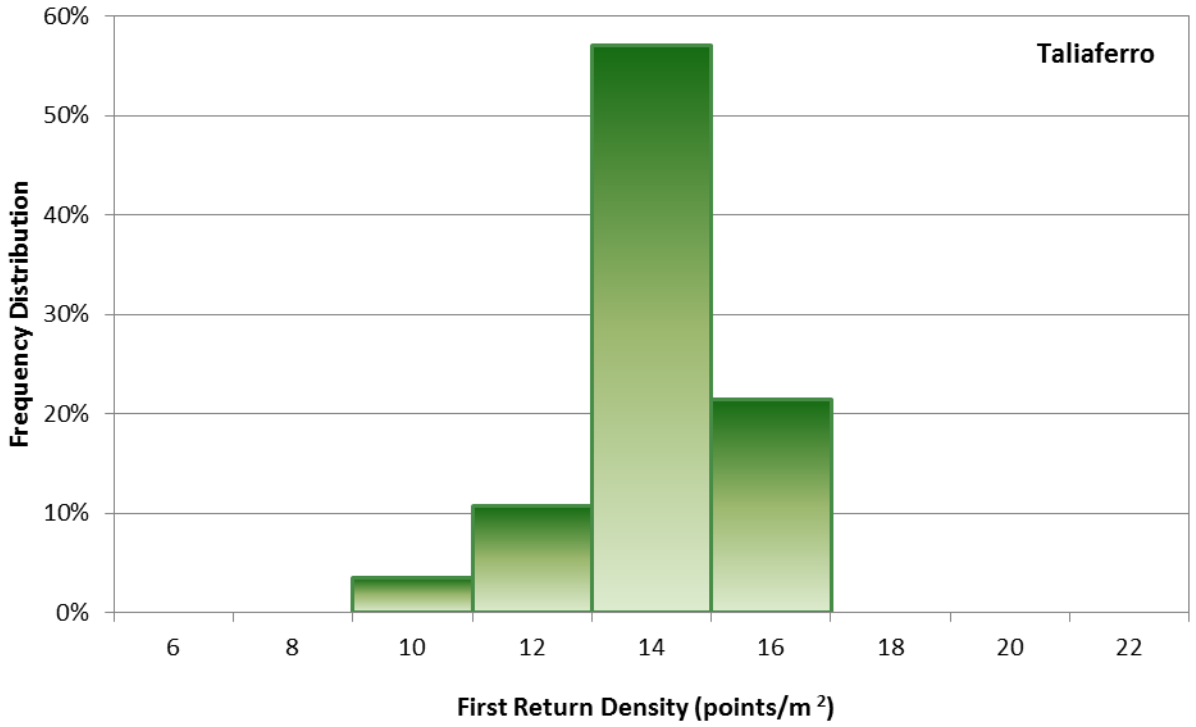


**Frequency distribution of first return densities (native densities) of the 1m gridded study area for the Taliaferro AOI**

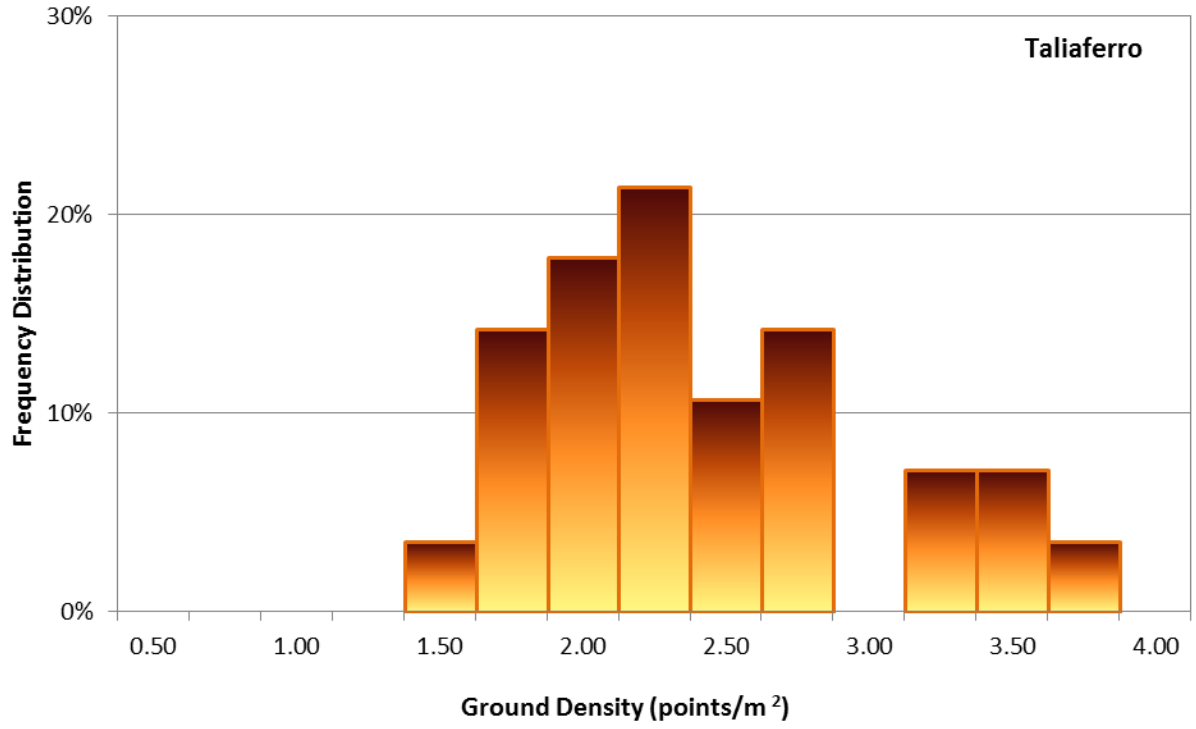


**Frequency distribution of ground return densities of the 1m gridded study area for the Taliaferro AOI**

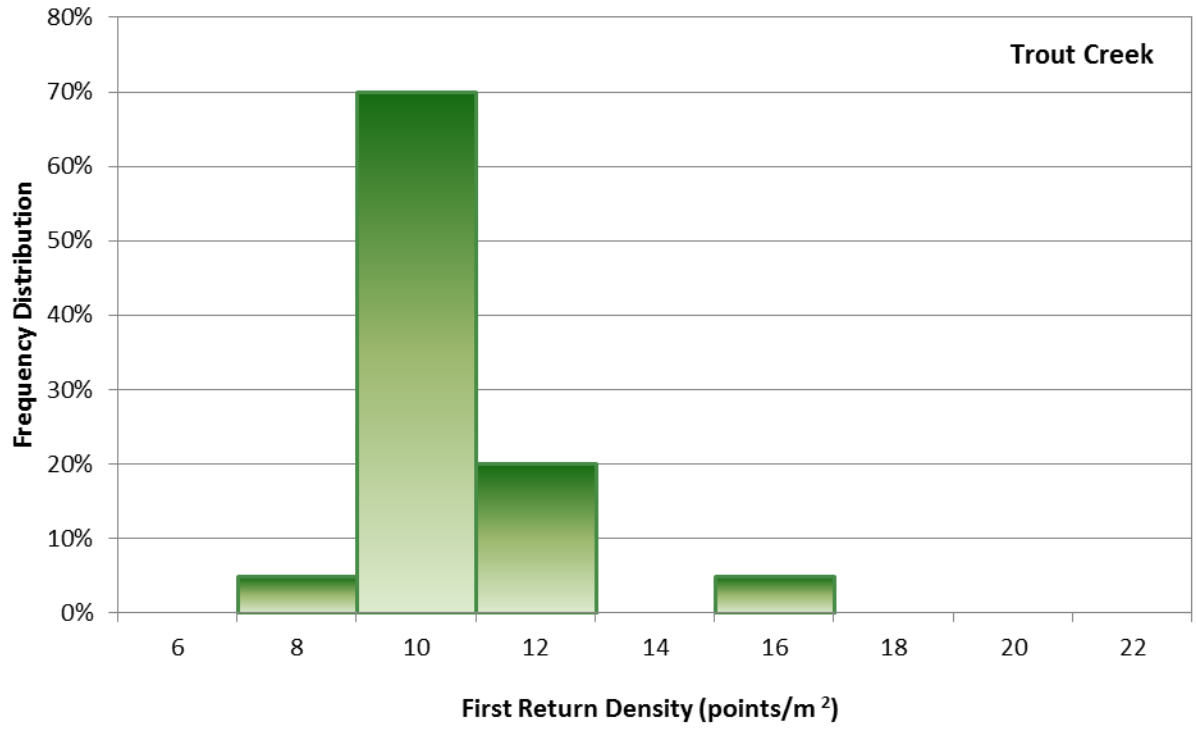


**Frequency distribution of first return densities (native densities) of the 1m gridded study area for the Trout AOI**

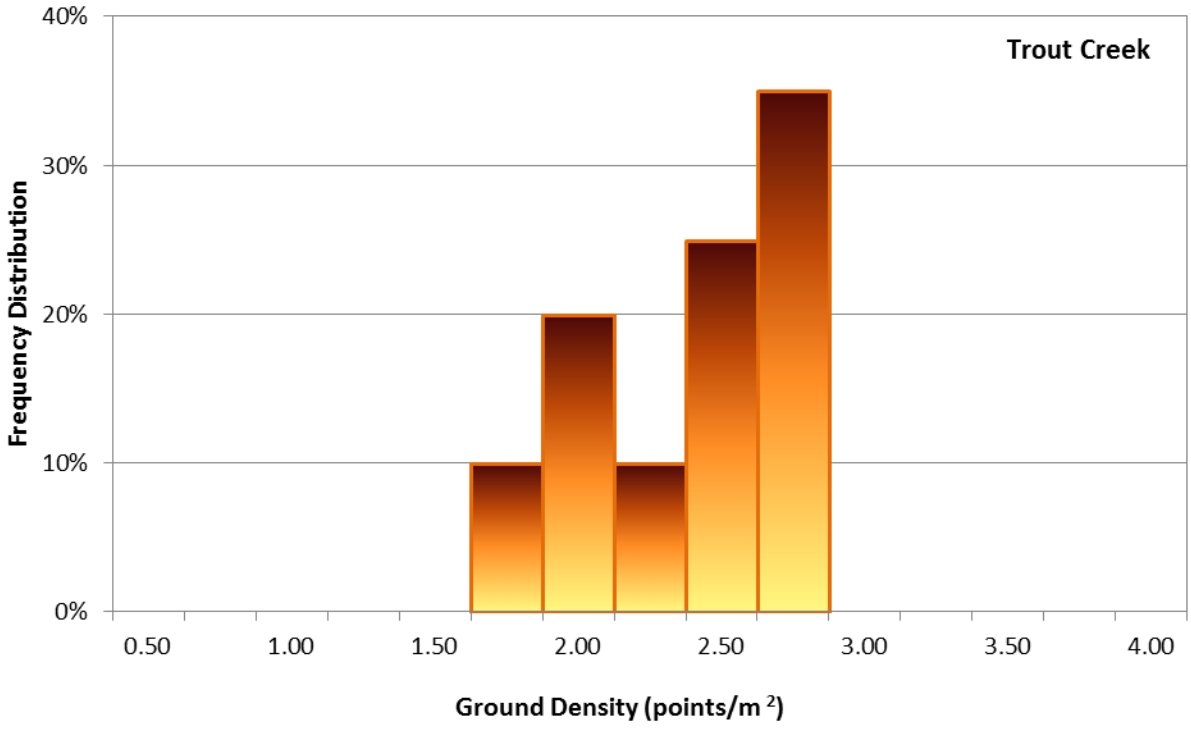


**Frequency distribution of ground return densities of the 1m gridded study area for the Trout AOI**

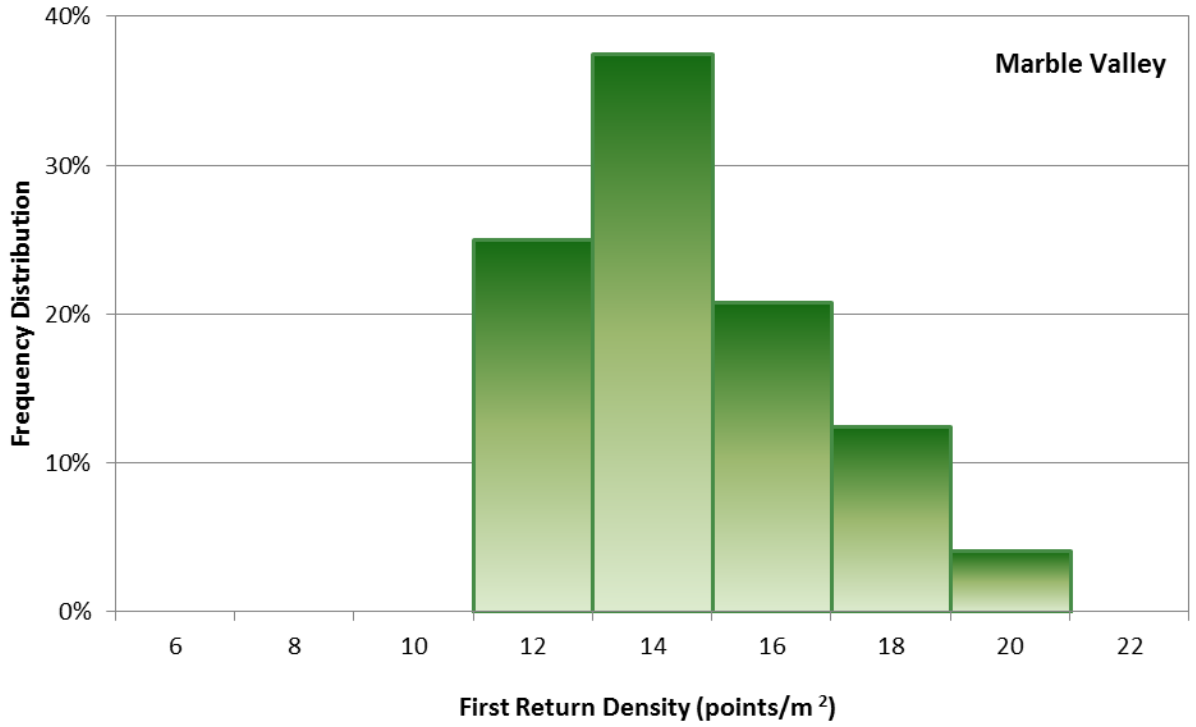


**Frequency distribution of first return densities (native densities) of the 1m gridded study area for the Marble Valley AOI**

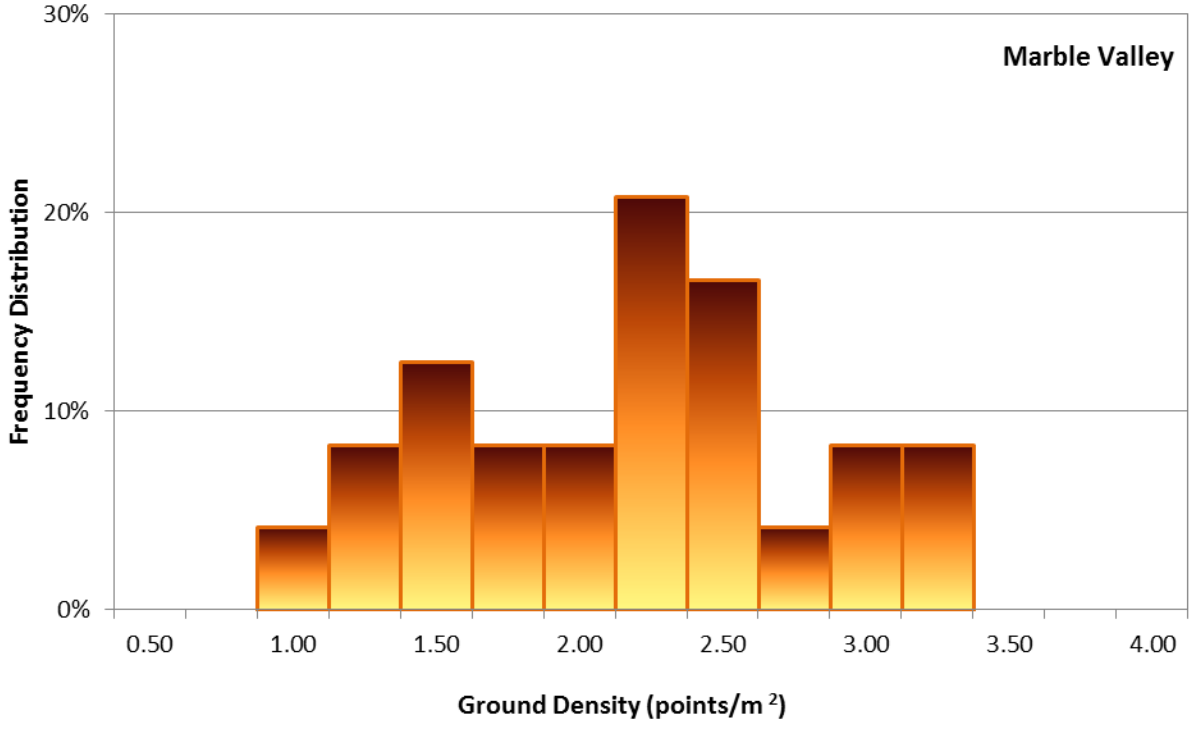


**Frequency distribution of ground return densities of the 1m gridded study area for the Marble Valley AOI**

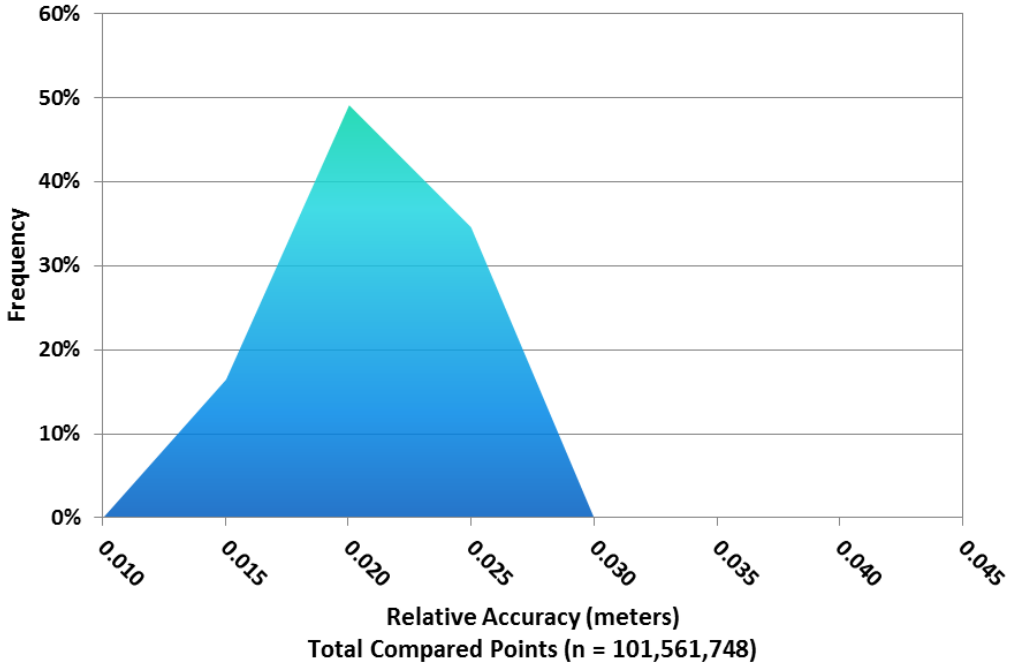


**Frequency plot for relative accuracy between flight lines for the Snag Hill AOI**

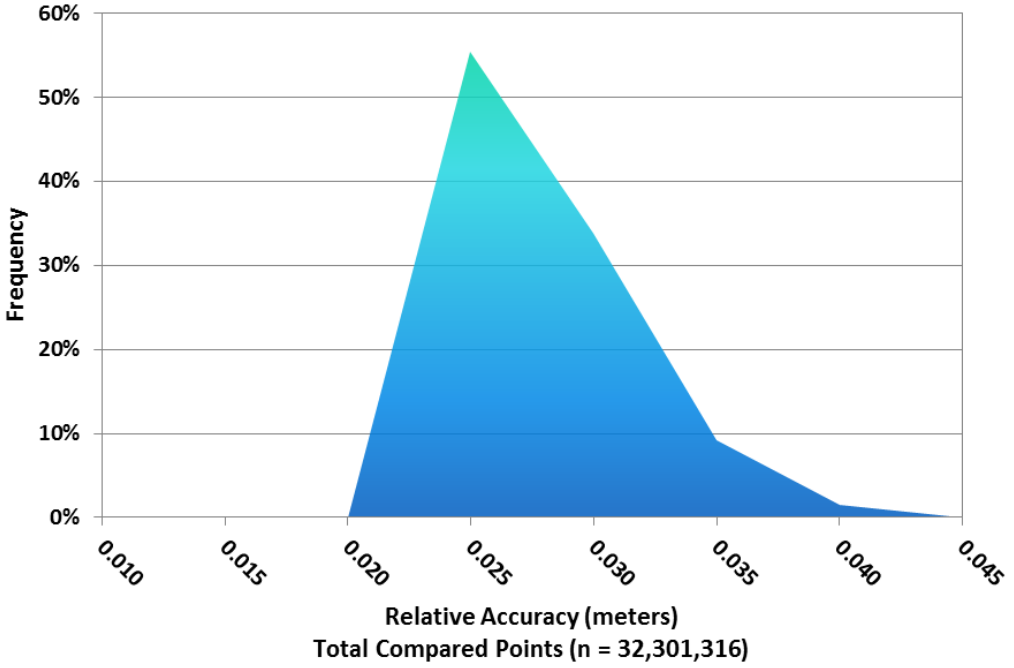


**Frequency plot for relative accuracy between flight lines for the Mule AOI**

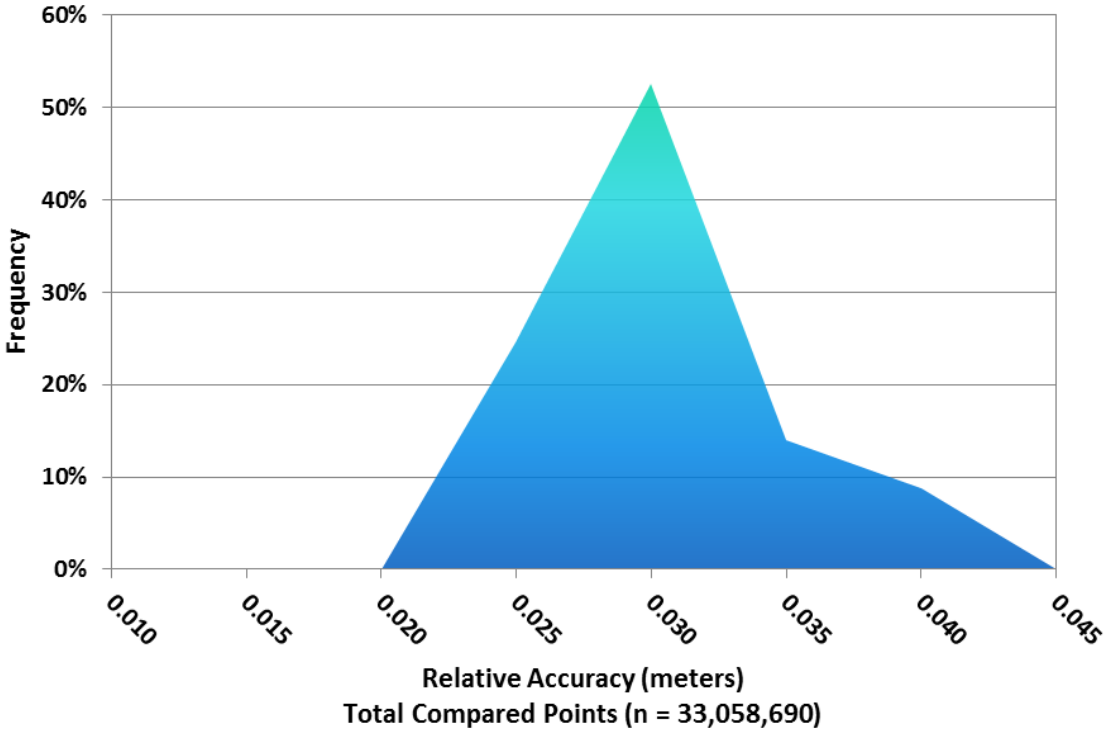


**Frequency plot for relative accuracy between flight lines for the Taliaferro AOI**

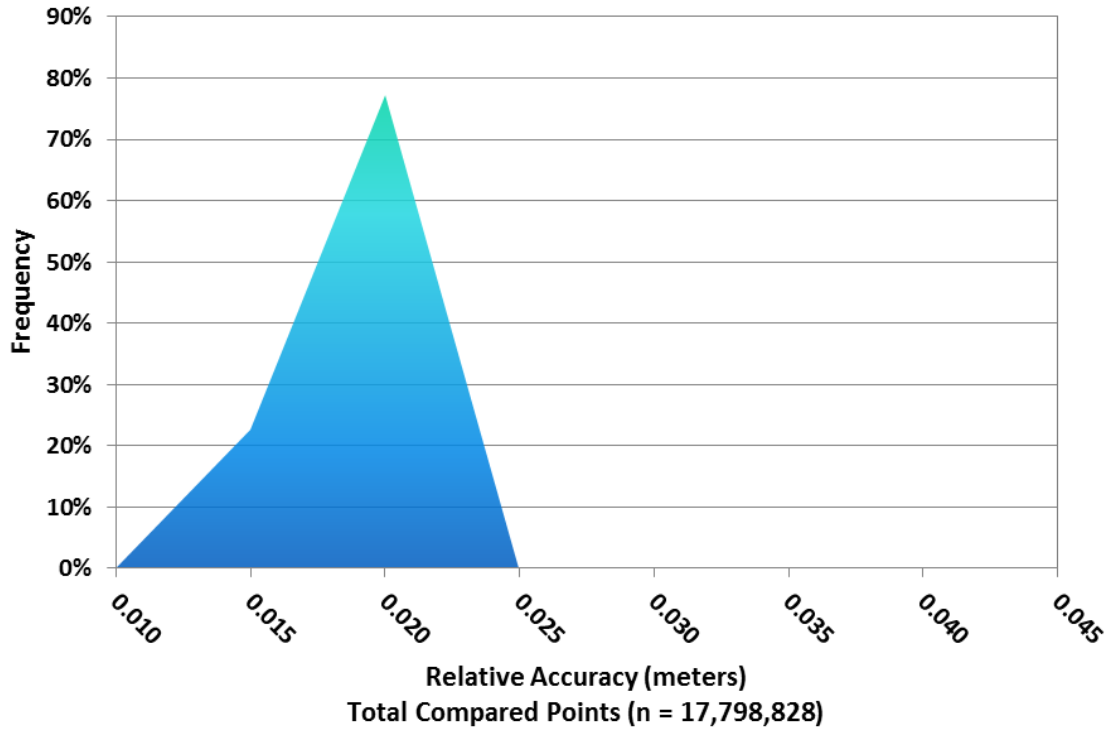


**Frequency plot for relative accuracy between flight lines for the Trout Creek AOI**

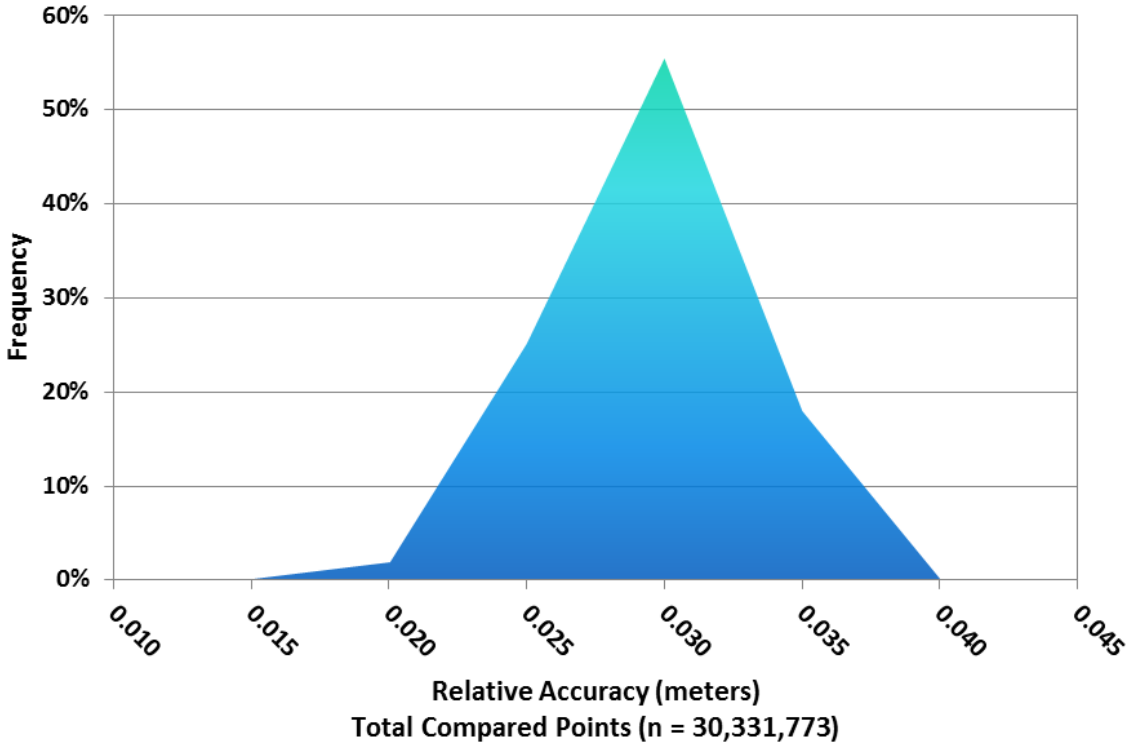


**Frequency plot for relative accuracy between flight lines for the Marble Valley AOI**

**Laser Noise**

For any given target, laser noise is the breadth of the data cloud per laser return (i.e., last, first, etc.). Lower intensity surfaces (roads, rooftops, still/calm water) experience higher laser noise. The laser noise range for this survey was approximately 0.02 meters.

**Relative Accuracy**

Relative accuracy refers to the internal consistency of the data set - the ability to place a laser point in the same location over multiple flight lines, GPS conditions, and aircraft attitudes. Affected by system attitude offsets, scale, and GPS/IMU drift, internal consistency is measured as the divergence between points from different flight lines within an overlapping area. Divergence is most apparent when flight lines are opposing. When the LiDAR system is well calibrated, the line-to-line divergence is low (<10 cm).

**Relative Accuracy Calibration Methodology**

Manual System Calibration: Calibration procedures for each mission require solving geometric relationships that relate measured swath-to-swath deviations to misalignments of system attitude parameters. Corrected scale, pitch, roll and heading offsets were calculated and applied to resolve misalignments. The raw divergence between lines was computed after the manual calibration was completed and reported for each survey area.

Automated Attitude Calibration: All data were tested and calibrated using TerraMatch automated sampling routines. Ground points were classified for each individual flight line and used for line-to-line testing. System misalignment offsets (pitch, roll and heading) and scale were solved for each individual mission and applied to respective mission datasets. The data from each mission were then blended when imported together to form the entire area of interest.

Automated Z Calibration: Ground points per line were used to calculate the vertical divergence between lines caused by vertical GPS drift. Automated Z calibration was the final step employed for relative accuracy calibration.

**Absolute Accuracy**

The vertical accuracy of LiDAR data is described as the mean and standard deviation (sigma σ) of divergence of LiDAR point coordinates from RTK ground survey point coordinates. To provide a sense of the model predictive power of the dataset, the root mean square error (RMSE) for vertical accuracy is also provided. These statistics assume the error distributions for x, y, and z are normally distributed, thus we also consider the skew and kurtosis of distributions when evaluating error statistics.

**LiDAR accuracy error sources and solutions:**

| Type of Error | Source | Post Processing Solution |
|---|---|---|
| **GPS (Static/Kinematic)** | Long Base Lines | None |
| | Poor Satellite Constellation | None |
| | Poor Antenna Visibility | Reduce Visibility Mask |
| **Relative Accuracy** | Poor System Calibration | Recalibrate IMU and sensor offsets/settings |
| | Inaccurate System | None |
| **Laser Noise** | Poor Laser Timing | None |
| | Poor Laser Reception | None |
| | Poor Laser Power | None |
| | Irregular Laser Shape | None |

**Operational measures taken to improve relative accuracy:**

Low Flight Altitude: Terrain following is employed to maintain a constant above ground level (AGL). Laser horizontal errors are a function of flight altitude above ground (i.e., ~ 1/3000$^{th}$ AGL flight altitude).

Focus Laser Power at narrow beam footprint: A laser return must be received by the system above a power threshold to accurately record a measurement. The strength of the laser return is a function of laser emission power, laser footprint, flight altitude and the reflectivity of the target. While surface reflectivity cannot be controlled, laser power can be increased and low flight altitudes can be maintained.

Reduced Scan Angle: Edge-of-scan data can become inaccurate. The scan angle was reduced to a maximum of ±15$^{o}$ from nadir, creating a narrow swath width and greatly reducing laser shadows from trees and buildings.

Quality GPS: Flights took place during optimal GPS conditions (e.g., 6 or more satellites and PDOP [Position Dilution of Precision] less than 3.0). Before each flight, the PDOP was determined for the survey day. During all flight times, a dual frequency DGPS base station recording at 1–second epochs was utilized and a maximum baseline length between the aircraft and the control points was less than 19 km (11.5 miles) at all times.

Ground Survey: Ground survey point accuracy (i.e. <1.5 cm RMSE) occurs during optimal PDOP ranges and targets a minimal baseline distance of 4 miles between GPS rover and base. Robust statistics are, in

part, a function of sample size (n) and distribution. Ground survey RTK points are distributed to the extent possible throughout multiple flight lines and across the survey area.

50% Side-Lap (100% Overlap): Overlapping areas are optimized for relative accuracy testing. Laser shadowing is minimized to help increase target acquisition from multiple scan angles. Ideally, with a 50% side-lap, the most nadir portion of one flight line coincides with the edge (least nadir) portion of overlapping flight lines. A minimum of 50% side-lap with terrain-followed acquisition prevents data gaps.

Opposing Flight Lines: All overlapping flight lines are opposing. Pitch, roll and heading errors are amplified by a factor of two relative to the adjacent flight line(s), making misalignments easier to detect and resolve.